ChemComm

COMMUNICATION

Efficient temperature-feedback liposome for ^{19}F MRI signal enhancement†

Cite this: *Chem. Commun.*, 2020, **56**, 14427

Received 27th August 2020,
Accepted 25th October 2020

DOI: 10.1039/d0cc05809b

rsc.li/chemcomm

Lili Ren,‡[ab] Shizhen Chen,‡*[a] Weiping Jiang,[a] Qingbin Zeng,[a] Xu Zhang,[a] Long Xiao,[a] Michael T. McMahon,[c] Lou Xin[d] and Xin Zhou *[a]

A new non-encapsulated fluorinated liposome (TSL) was developed, which showed instantaneous temperature-induced ^{19}F MR signal enhancement and excellent stability under reversible signal transition at different conditions.

^{19}F labeling has emerged as an attractive new option for creating MRI imaging agents. ^{19}F MRI allows for the specific detection of imaging agents due to the absence of endogenous fluorine in the body, thereby avoiding the need for pre-scans, and removing localization ambiguities that were present when ^{1}H relaxation based imaging agents were employed.[1] The gyromagnetic ratio of ^{19}F (40.05 MHz T^{-1}) is very similar to that of ^{1}H (42.58 MHz T^{-1}), and allows for high sensitivity detection and the use of the same experimental setup to detect both ^{19}F and ^{1}H signals, with the same receiver electronics but retuned radiofrequency coils.[2] Because of these advantages, ^{19}F agents have been developed for a wide range of possible applications.

^{19}F MRI probes have been applied in tumor imaging, detection of hypoxia, tissue imaging, cellular imaging, pH measurements, monitoring of enzymatic activity and more.[3] However, in most cases, it is a challenge to apply ^{19}F probes *in vivo* because of the poor water solubility, biocompatibility, and insufficient amounts of fluorine.[4] Linear fluorinated compounds provide more than one resonance frequency.[5] Multiple fluorine resonances lead to low signal intensity, requiring even higher concentrations to obtain sufficient signal strength for detection. Symmetric compounds are difficult to modify.[5] The most widely used perfluorinated contrast agents, perfluorocarbons (PFCs) and perfluoropolyethers (PFPEs), excessively accumulate in internal organs. Studies have shown that perfluorocarbon-hydrocarbon mixtures nearly cannot easily be metabolized, and perfluoro-crown-ethers are retained in the liver for as long as 25 days. In addition, these compounds have shown poor pharmacokinetics in rats, which leaves room for substantial improvement.[2,3] Thus, the application of ^{19}F imaging agents is limited.

Fluorine-labeled liposomes may help solve the above-mentioned problems. Liposomes, which can entrap hydrophilic and hydrophobic agents or molecules, are a type of nano-carrier used for *in vivo* applications.[6] The liposomal drug carrier Doxil® is currently used for treating patients with ovarian cancer or Karposi Sarcoma. Several other liposomal formulations are currently in clinical trials.[7] Liposomal encapsulation of pharmaceuticals is performed to reduce undesirable side effects and protect them from inactivation by external factors. Incorporation of polyethylene glycol (PEG) will prolong the circulation time. The properties and function of liposome can be easily modified by changing the blend of lipids and sterols prior to self-assembly.[7] For example, multilayered lipid-based nanocarriers loaded with perfluorohexane (PFH) or perfluoro-15-crown-5-ether (PFCE)/ovalbumin (OVA) can be used to track dendritic cells (DCs) and activate and proliferate antigen-specific CD8+ T cells efficiently *in vitro*. The labeled cells can be imaged by ^{19}F MRI.[8] Temperature-sensitive liposomes with a ^{19}F MRI probe NH_4PF_6 and a paramagnetic shift agent [Tm(hpdo3a)(H_2O)] entrapped, provide switchable MRI signals, when the ^{19}F NMR signal is switched from the off to on position above 311 K, which allows for the detection of drug release after localized heating.[9] Nanoparticle-incorporated fluorine groups can enhance the fluoride concentration due to their large molecular weight, reduce relaxation times by virtue of their size or the presence of paramagnetic ions, and thereby increase the signal-to-noise ratio.[6]

[a] *Key Laboratory of Magnetic Resonance in Biological Systems, State Key Laboratory of Magnetic Resonance and Atomic and Molecular Physics, National Center for Magnetic Resonance in Wuhan, Wuhan Institute of Physics and Mathematics, Innovation Academy for Precision Measurement Science and Technology, Chinese Academy of Sciences, Wuhan National Laboratory for Optoelectronics, 430071, Wuhan, China. E-mail: xinzhou@wipm.ac.cn, chenshizhen@wipm.ac.cn*

[b] *Department of Pulmonary and Critical Care Medicine, The Second Affiliated Hospital of Xi'an Jiaotong University, Xi'an, China*

[c] *Russell H. Morgan Department of Radiology and Radiological Science, The Johns Hopkins University School of Medicine, F.M. Kirby Research Center for Functional Brain Imaging Kennedy Krieger Institute Baltimore, Maryland 21287, USA*

[d] *Department of Radiology, Chinese PLA General Hospital, Beijing, China*

† Electronic supplementary information (ESI) available: Synthesis of compounds, preparation, characterizations and studies of TSL. See DOI: 10.1039/d0cc05809b

‡ Lili Ren and Shizhen Chen contributed equally to this work.

Here, we have developed a type of non-encapsulated fluorinated temperature-sensitive liposome (TSL) for self-quenching and reversible off/on ^{19}F MRI to greatly improve the accuracy and sensitivity of tumor detection. The newly synthetic fluorinated lipid (F-PC) can satisfy the demands of two image modes (^{19}F MRI and fluorescence imaging) and has good biocompatibility. The lipid tag-labeled liposome has an efficient reversible temperature response, good utilization properties by repeated sample usage, and is stable at body temperature. Together with enhanced permeability and retention effect (EPR) of nanocarriers and controlled localized heating, the uptake of liposomes by tumor cells *via* endocytosis was increased.[10] The accuracy and sensitivity of TSL will be greatly enhanced. Furthermore, the direct conjugation of fluorine and fluorophore on lipids solves the problem of differential distribution, which may occur if fluorine and fluorophore were merely encapsulated. The empty core of liposomes can carry other functional hydrophilic substances, including anticancer drugs, thereby increasing the application of non-encapsulated fluorinated liposomes (Fig. 1).

Fluorinated and fluorescent lipids (F-PC) were synthesized as shown in Fig. S1 (ESI†).[11] For each product, ^{1}H/^{13}C/^{19}F NMR and HRMS were recorded to determine the preparation of correct compounds (ESI†). F-PC shows one single sharp peak at −62.60 ppm (Fig. 2a). The T_1 and T_2 of the solutions of F-PC (5.7 mM in $CHCL_3$–$CDCL_3$) were 1.012 s and 185.8 ms, respectively. The fluorescence spectra obtained revealed that the maximum excitation and emission wavelengths of F-PC were 370 nm and 425 nm, respectively (Fig. 2b). The hydrodynamic diameter, polymer dispersity index (PDI) and zeta potential of F-PC-labeled TSL were 185.1 nm (Fig. 2c), 0.178, and −9.1 at 25 °C, respectively. TSL water solution was emulsible (Fig. 2d(1)) and blue fluorescence (Fig. 2d(2)). Large TSLs were taken during the generation of TSL and imaged by CLSM, which was indicated by a blue ring representing the F-PC-labeled liposome with fluorine inside the bilayer (Fig. 2d(3)).

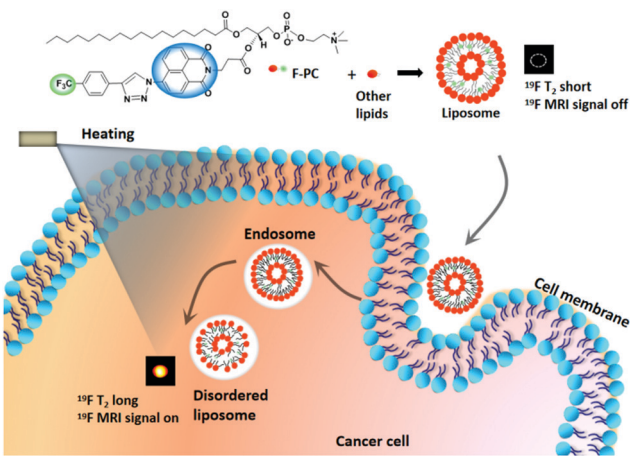

Fig. 1 Structure of newly synthetic fluorinated lipid (F-PC). The blue and green parts can be applied for fluorescence imaging and ^{19}F MRI, respectively. Temperature-sensitive liposomes (TSLs) can accumulate in tumors by enhanced permeability and retention effect (EPR) and temperature-controlled stabilization and are mainly taken up by tumor cells *via* the process of endocytosis, followed by the detection by ^{19}F MRI from off to on at a mild temperature (37–42 °C).

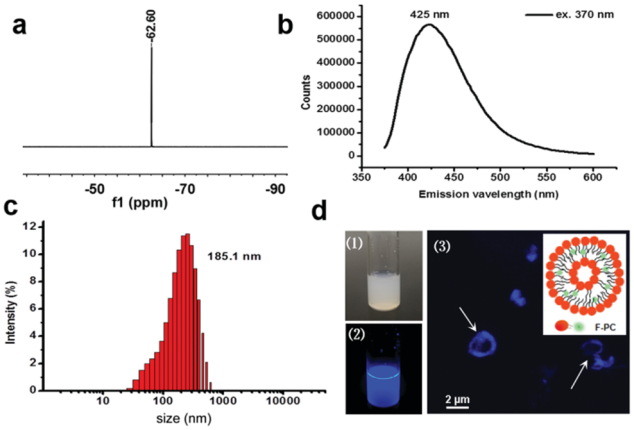

Fig. 2 (a) ^{19}F NMR of F-PC in $CDCl_3$. (b) Fluorescence spectrum of F-PC in CHCL3. (c) The intensity of liposome diameters and their average size in water as measured by dynamic light scattering (DLS). (d) Pictures of TSL water solution under white light (1) and fluorescent light (2), fluorescence images of large TSL by CLSM (3), with white arrows showing the obvious annular non-encapsulated F-PC labeled liposome, insert: structure diagram of TSL.

When increasing the temperature, no evident variation in size or PDI of TSLs was observed (Fig. 3a). The spherical particles were visualized by TEM before (Fig. 3b(1)) and after (Fig. 3b(2)) incubation at high temperature (42 °C), which showed that there was no distinct variation of liposomal appearance above the phase transition temperature. Some partial changes in the microstructure could have taken place during the transition from the organized gel phase to the disorganized fluid phase at a high temperature. The ^{19}F signal could not be observed at room temperature. After adding the surfactant (5% Triton X-100), a single ^{19}F peak appeared as the broken of liposomal structure (data not shown), when the fluorine content was about 18 μmol mg^{-1} of liposome. Different from metal ions induced ^{19}F signal off,[1,3,9,12] this TSL has a self-quenching signal of ^{19}F when the F-PC-tagged liposome is formed. In the "off" state, the ^{19}F signal might be suppressed due to limited rotation of the fluorine group.[13]

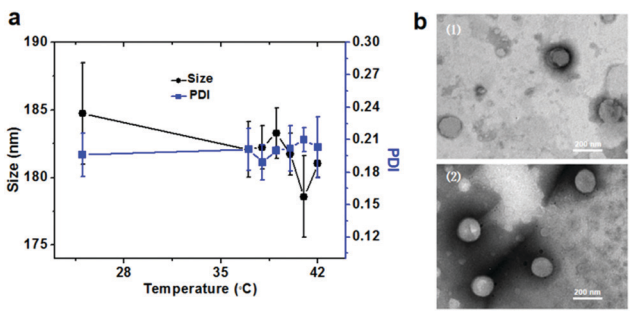

Fig. 3 (a) Size and PDI variation of TSL at different temperatures. Experiments were performed in triplicate. (b) TEM images of TSL at 25 °C (1) and 42 °C (2).

In this study, unique ^{19}F NMR signal responses were tested at a mild temperature. There was no ^{19}F NMR signal of fluorinated liposomes at 25 °C or 37 °C, thereby indicating the intact structure of TSLs at experimental conditions or at a physiological temperature. The ^{19}F NMR signal (−62.47 ppm) appeared at a temperature of 39 °C and increased with an increasing temperature (Fig. 4a). The integrated signal at 42 °C was nearly as strong as that of Triton-X lysed TSL (Fig. S2a, ESI†). Furthermore, as shown in the time course in Fig. 4b, the ^{19}F NMR signal could be detected at 1 min after heating to 42 °C and the integrated signal was nearly identical as that of control group (Fig. S2b, ESI†), showing a fast response rate and a high response efficiency. Furthermore, the ^{19}F NMR signal could be detected at a concentration of 0.18 mM fluorine of liposome (10 mg ml^{-1}). The signal increased with increasing concentrations of TSL (Fig. S3, ESI†). Unlike other encapsulated or responsive agents, TSL had the unique feature that the ^{19}F MR signal switch was reversible. The ^{19}F signal of TSL in a water solution was in the "off" phase at 37 °C and in the "on" state when heated to 42 °C. After 6 cycles of heating to 42 °C and cooling to 37 °C, the ^{19}F signal could still be turned on at 42 °C (Fig. 4c). Because the hydrophobic fluorine part was located inside the bilayer, the ^{19}F NMR signal intensity was too low to be detected due to the short T_2, indicating the self-quencher ability of TSL as a ^{19}F MRI imaging agent.[13] When the temperature was raised above 39 °C, about the phase transition temperature of the lipids, the liposomal structure became destabilized, which increased T_2 and also the apparent ^{19}F NMR signal. Based on the TEM results and F-PC structure, a disrupted TSL at a moderately high temperatures might re-assemble when the TSL is cooled.

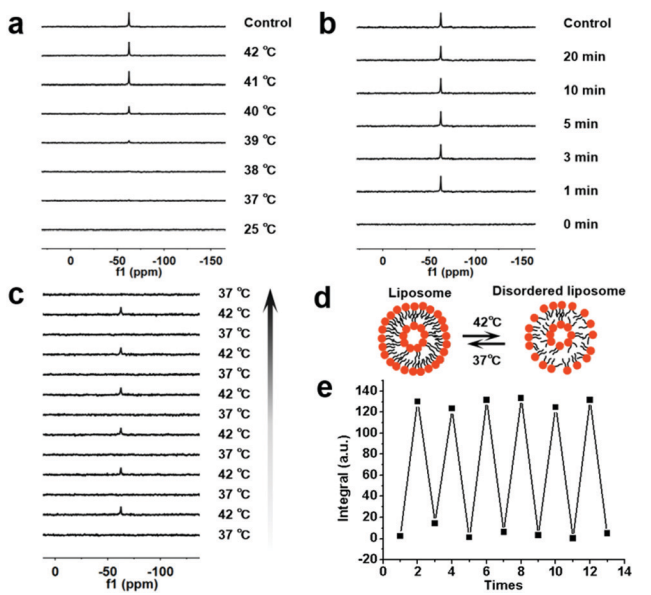

Fig. 4 (a) ^{19}F NMR of TSL for 25, 37, 38, 39, 40, 41 and 42 °C, Triton-X lysed TSL as the control. (b) ^{19}F NMR of TSL at 0, 1, 3, 5, 10, and 20 min after warming TSL to 42 °C, with Triton-X lysed TSL as the control. (c) Reversible ^{19}F NMR of TSL after repeated warming and cooling cycles at 42 °C and 37 °C. (d) Possible structural representation of TSL at low and high temperatures. (e) Integral curve of ^{19}F NMR signal corresponding to c.

The performance of molecule-encapsulated TSL was different from that of non-encapsulated TSL. The ^{19}F NMR signal of perfluorooctyl bromide (PFOB)-encapsulated TSL(PFOB-TSL), which was prepared using a process that was similar as that of TSL and about 183.6 nm, was always in the "on" state, both at low or high temperatures, and was a bit attenuated at a high temperature (Fig. S4, ESI†). As different chemical environment of fluorine, there was more than one resonance frequency of PFOB, which might induce chemical shift artifacts.[3] TSL only had one fluorine signal, which made it easier to detect by MRI. Combined with the ^{19}F NMR signal, the size and TEM analysis of TSL at different temperatures, the actions of encapsulated compounds and tagged lipids might be different when the temperature increases above the phase transition point. Different from always "on" mode of encapsulated PFOB, a relative stable and controllable fluorinated lipid-labeled TSL could be used as a signal "off" to "on" using ^{19}F MRI contrast agent.

A reversible ordered closed and disordered open state of the TSL at low and high temperatures might correspond to a ^{19}F NMR signal in the "off" and "on" states (Fig. 4d). The strength of the ^{19}F signal at 42 °C after the sixth heating was almost identical to that of the first heating, thus, maintaining a consistent reversible response over at least 6 cycles (Fig. 4e). This reversible performance was found to be maintained in more complicated conditions, such as in serum (Fig. S5, ESI†) or in cell lysates (Fig. S6, ESI†). To our knowledge, this type of excellent reversible fluorine imaging agent has not yet been reported. These properties greatly improved the stability of the TSL at body temperature, and therefore, are promising for improving the imaging efficiency *in vivo*.

Fluorescence imaging and ^{19}F MRI could be performed by TSL. Blue F-PC-labeled liposomes were readily endocytosed by A549 cells, and were mainly located in the cytoplasm according to the fluorescence data (Fig. 5a). Direct conjugation of fluorine and fluorescence labels to lipid solves the problem of not knowing if these are in the same or different compartments, which may occur when two components are merely co-encapsulated.[4] ^{19}F MRI can readily be performed when TSLs are present in water or a more complicated cell lysates without any ambiguity (Fig. 5b). ^{19}F

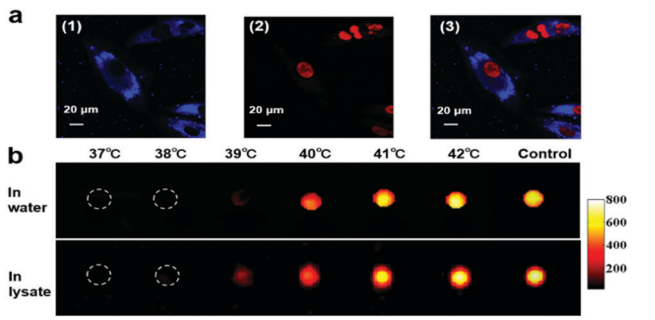

Fig. 5 (a) Fluorescence image of A549 cells incubated with TSL. The blue channel (1), red channel (2) and merge (3) of (1) and (2). The blue color represents TSL. Red indicates the cell nucleus stained with RedDot. (b) ^{19}F MRI of TSL in water or cell lysates at different temperatures. TSL with Triton-X was the control group.

MRI signal was detected when the temperature was above 39 °C, increased with increasing temperature, and was nearly identical as the Triton-X control group at around 42 °C. These results indicated the possibility of applying TSL in *in vivo* studies using localized heating.

In summary, we successfully developed a new non-encapsulated fluorinated and reversible off/on ^{19}F MRI imaging agent with good solubility and polydispersity. The ^{19}F NMR/MRI signal is turned ''on'' at mild temperatures (around 42 °C) in a fast and efficient manner. This stimuli-sensitive liposome has emerged as a novel responsive ^{19}F MR system in which the MR signal can be controlled at the slightly higher temperature of tumor tissue when compared to healthy tissues. Furthermore, TSL has a fluorescence probe incorporated to allow for histological detection. The special repetitive reversible ^{19}F off/on signal properties displayed outstanding stability over a wide range of *in vitro* conditions, including water, serum and cell lysates. The TSL takes advantage of the EPR (enhanced permeability and retention) effect of tumors with incorporated PEG to prolong their circulation time, and might be appropriate for using the ^{19}F signal to detect tumor and monitor release of therapeutics in locally-heated tumors.[14] Finally, this F-PC could be readily incorporated into other lipid-based or amphiphilic nanocarriers to add ^{19}F MRI and fluorescence capabilities.

We are thankful for financial support from National Key R&D Program of China (2018YFA0704000), National Natural Science Foundation of China (81801690, 81625011, 91859206, 21874150, 81730048, 81825012), Key Research Program of Frontier Sciences, CAS (ZDBS-LY-JSC004, QYZDY-SSW-SLH018) and Hubei Provincial Natural Science Foundation of China (2017 CFA013, 2018ACA143). Xin Zhou acknowledges the support from the Tencent Foundation through the XPLORER PRIZE. Human lung adenocarcinoma cell line A549 cell line was obtained from the Cell Bank of Chinese Academy of Sciences (Shanghai, China).

Conflicts of interest

There are no conflicts to declare.

Notes and references

1 (*a*) S. Mizukami, R. Takikawa, F. Sugihara, Y. Hori, H. Tochio, M. Wälchli, M. Shirakawa and K. Kikuchi, *J. Am. Chem. Soc.*, 2008, **130**, 794; (*b*) J. Cui, R. Jiang, C. Guo, X. Bai, S. Xu and L. Wang, *J. Am. Chem. Soc.*, 2018, **140**, 5890; (*c*) K. L. Peterson, K. Srivastava and V. C. Pierre, *Front. Chem.*, 2018, **6**, 160.

2 (*a*) H. Amiri, M. Srinivas, A. Veltien, M. J. van UdenI and J. M. de VriesArend Heerschap, *Eur. Radiol.*, 2015, **25**, 726; (*b*) J. Ruiz-Cabello, B. P. Barnett, P. A. Bottomley and J. W. M. Bulte, *NMR Biomed.*, 2011, **24**, 114; (*c*) M. Srinivas, A. Heerschap, E. T. Ahrens, C. G. Figdor and I. J. M. de Vries, *Trends Biotechnol.*, 2010, **28**, 363; (*d*) J. X. Yu, R. R. Hallac, S. Chiguru and R. P. Mason, *Prog. Nucl. Mag. Res. Sp.*, 2013, **70**, 25; (*e*) R. Pujales-Paradela, T. Savić, I. Brandariz, P. Pérez-Lourido, G. Angelovski, D. Esteban-Gómez and C. Platas-Iglesias, *Chem. Commun.*, 2019, **55**, 4115.

3 (*a*) S. Hunjan, R. P. Mason, V. D. Mehta, P. V. Kulkarni, S. Aravind, V. Arora and P. P. Antich, *Magn. Reson. Med.*, 1998, **39**, 551; (*b*) K. Tanabe, H. Harada, M. Narazaki, K. Tanaka, K. Inafuku, H. Komatsu, T. Ito, H. Yamada, Y. Chujo, Y. Matsuda, M. Hiraoka and S. Nishimoto, *J. Am. Chem. Soc.*, 2009, **131**, 15982; (*c*) I. Tirotta, A. Mastropietro, C. Cordiglieri, L. Gazzera, F. Baggi, G. Baselli, M. G. Bruzzone, I. Zucca, G. Cavallo, G. Terraneo, F. B. Bombelli, P. Metrangolo and G. Resnati, *J. Am. Chem. Soc.*, 2014, **136**, 8524; (*d*) S. Mizukami, R. Takikawa, F. Sugihara, M. Shirakawa and K. Kikuchi, *Angew. Chem., Int. Ed.*, 2009, **48**, 3641; (*e*) A. Bar-Shir, N. N. Yadav, A. A. Gilad, P. C. M. van Zijl, M. T. McMahon and J. W. M. Bulte, *J. Am. Chem. Soc.*, 2015, **137**, 78; (*f*) D. Xie, S. Kim, V. Kohli, A. Banerjee, M. Yu, J. S. Enriquez, J. J. Luci and E. L. Que, *Inorg. Chem.*, 2017, **56**, 6429; (*g*) S. Chen, Y. Yang, H. Li, X. Zhou and M. Liu, *Chem. Commun.*, 2014, **50**, 283.

4 (*a*) I. Tirotta, V. Dichiarante, C. Pigliacelli, G. Cavallo, G. Terraneo, F. B. Bombelli, P. Metrangolo and G. Resnati, *Chem. Rev.*, 2015, **115**, 1106; (*b*) K. J. Thurecht, I. Blakey, H. Peng, O. Squires, S. Hsu, C. Alexander and A. K. Whittaker, *J. Am. Chem. Soc.*, 2010, **132**, 5336; (*c*) J. M. Janjic, M. Srinivas, D. K. Kadayakkara and E. T. Ahrens, *J. Am. Chem. Soc.*, 2008, **130**, 2832; (*d*) E. T. Ahrens, B. M. Helfer, C. F. O'hanlon and C. Schirda, *Magn. Reson Med.*, 2014, **72**, 1696; (*e*) C. Constantinides, M. L. Maguire, L. Stork, E. Swider, M. Srinivas, C. A. Carr and J. E. Schneider, *J. Magn. Reson. Imaging*, 2017, **45**, 1659.

5 (*a*) W. Du, A. M. Nyström, L. Zhang, K. T. Powell, Y. Li, C. Cheng, S. A. Wickline and K. L. Wooley, *Biomacromolecules*, 2008, **9**, 2826; (*b*) C. Zhang, S. S. Moonshi, Y. Han, S. Puttick, H. Peng, B. J. A. Magoling, J. C. Reid, S. Bernardi, D. J. Searles, P. Král and A. K. Whittaker, *Macromolecules*, 2017, **50**, 5953.

6 (*a*) M. P. Placidi, M. Botta, F. K. Kálmán, G. E. Hagberg, Z. Baranyai, A. Krenzer, A. K. Rogerson, I. Tóth, N. K. Logothetis and G. Angelovski, *Chem. – Eur. J.*, 2013, **19**, 11644; (*b*) L. Ren, S. Chen, H. Li, Z. Zhang, J. Zhong, M. Liu and X. Zhou, *Acta Biomater.*, 2016, **35**, 260; (*c*) L. Ren, S. Chen, H. Li, Z. Zhang, C. Ye, M. Liu and X. Zhou, *Nanoscale*, 2015, **7**, 12843; (*d*) Y. Liu and N. Zhang, *Biomaterials*, 2012, **33**, 5363; (*e*) W. T. Al-Jamal and K. Kostarelos, *Acc. Chem. Res.*, 2011, **44**, 1094; (*f*) Y. Chen, A. Bose and G. D. Bothun, *ACS Nano*, 2010, **4**, 3215; (*g*) C. Grange, S. Geninatti-Crich, G. Esposito, D. Alberti, L. Tei, B. Bussolati, S. Aime and G. Camussi, *Cancer Res.*, 2010, **70**, 2180.

7 V. P. Torchilin, *Nat. Rev. Drug Discovery*, 2005, **4**, 145.

8 H. Dewitte, B. Geers, S. Liang, U. Himmelreich, J. Demeester, S. C. De Smedt and I. Lentacker, *J. Control. Release*, 2013, **169**, 141.

9 S. Langereis, J. Keupp, J. L. J. van Velthoven, I. H. C. de Roos, D. Burdinski, J. A. Pikkemaat and H. Grüll, *J. Am. Chem. Soc.*, 2009, **131**, 1380.

10 (*a*) D. I. Piraner, M. H. Abedi, B. A. Moser, A. L. Gosselin and M. G. Shapiro, *Nat. Chem. Biol.*, 2017, **13**, 75; (*b*) F. Yan, S. Wang, W. Yang, S. Nahum Goldberg, H. Wu, W. L. Duan, Z. T. Deng, H. B. Han and H. R. Zheng, *Radiology*, 2017, **285**, 462; (*c*) P. Yingchoncharoen, D. S. Kalinowski and D. R. Richardson, *Pharmacol. Rev.*, 2016, **68**, 736.

11 (*a*) Y. Xia, F. Qu, A. Maggiani, K. Sengupta, C. Liu and L. Peng, *Org. Lett.*, 2011, **13**, 4248; (*b*) J. F. Lovell, C. S. Jin, E. Huynh, H. Jin, C. Kim, J. L. Rubinstein, W. C. W. Chan, W. Cao, L. V. Wang and G. Zheng, *Nat. Mater.*, 2011, **10**, 324; (*c*) S. Shao, J. Geng, H. A. Yi, S. Gogia, S. Neelamegham, A. Jacobs and J. F. Lovell, *Nat. Chem.*, 2015, **7**, 438; (*d*) W. Celentano, G. Neri, F. Distante, M. Li, P. Messa, C. Chirizzi, L. Chaabane, F. De Campo, P. Metrangolo, F. B. Bombelli and F. Cellesi, *Polym. Chem.*, 2020, **11**, 3951.

12 K. Akazawa, F. Sugihara, T. Nakamura, S. Mizukami and K. Kikuchi, *Bioconjugate Chem.*, 2018, **29**, 1720.

13 (*a*) K. Tanaka, N. Kitamura and Y. Chujo, *Bioconjugate Chem.*, 2011, **22**, 1484; (*b*) Z. Zheng, H. Sun, C. Hu, G. Li, X. Liu, P. Chen, Y. Cui, J. Liu, J. Wang and G. Liang, *Anal. Chem.*, 2016, **88**, 3363.

14 T. Tagami, W. D. Foltz, M. J. Ernsting, C. M. Lee, I. F. Tannock, J. P. May and S. D. Li, *Biomaterials*, 2011, **32**, 6570.

